

Electronic Supplementary Information

Spontaneous preparation of a fluorescent ratiometric chemosensor for metal ions using off-the-shelf materials

Yui Sasaki,^a Kohei Ohshiro,^a Qi Zhou,^a Xiaojun Lyu,^a Wei Tang,^a Kiyosumi Okabe,^a Shin-ya Takizawa^b and Tsuyoshi Minami*^a

^a Institute of Industrial Science, The University of Tokyo, 4-6-1 Komaba, Meguro-ku, Tokyo, 153-8505, Japan.

Corresponding author: tminami@g.ecc.u-tokyo.ac.jp

^b Department of Basic Science, Graduate School of Arts and Sciences, The University of Tokyo, 3-8-1, Komaba, Meguro-ku, Tokyo, 153-8902, Japan.

Contents

1. General	S2
2. UV-vis and fluorescence titrations of 3-NPBA	S3
3. Selected UV-vis titrations	S4
4. Selected fluorescence titrations	S8
5. Emission quantum yield and emission lifetime	S12
6. Discuss on a binding stoichiometry between EL and Pb ²⁺	S12
7. Semi-quantitative assay	S13
8. Real-sample analysis	S13
References	S13

1. General

Reagents

All reagents and samples were used without further purification. Esculetin (EL), potassium perchlorate (K^+), sodium perchlorate (Na^+), cesium chloride (Cs^+), and trace elements in river water (Elevated Level) were purchased from FUJIFILM Wako Pure Chemical Co. The target metal ions purchased from Sigma-Aldrich were cobalt(II) perchlorate hexahydrate (Co^{2+}), calcium perchlorate tetrahydrate (Ca^{2+}), lead(II) perchlorate trihydrate (Pb^{2+}), barium perchlorate trihydrate (Ba^{2+}), cadmium perchlorate hydrate (Cd^{2+}), nickel(II) perchlorate hexahydrate (Ni^{2+}), copper(II) perchlorate hexahydrate (Cu^{2+}), magnesium perchlorate hexahydrate (Mg^{2+}), zinc perchlorate hexahydrate (Zn^{2+}), and mercury(II) nitrate monohydrate (Hg^{2+}). 3-Nitrophenylbronic acid (3-NPBA) was purchased from Tokyo Chemical Industry Co., Ltd. 4-(2-hydroxyethyl)-1-piperazineethanesulfonic acid (HEPES) was purchased from Dojindo Laboratories Co., Ltd. HPLC grade methanol was obtained from Kanto Chemical Co., Inc. Milli-Q water ($18.2\text{ M}\Omega\cdot\text{cm}$) was utilized for the preparation of aqueous solutions.

Apparatuses

For evaluation of optical properties: The binding constants were estimated according to published methods.¹ UV-vis absorption spectra were recorded using a Shimadzu UV-2600 spectrophotometer within the wavelength range from 300 to 600 nm at 25 °C. A HITACHI F-7100 spectrophotometer was employed to record fluorescence spectra and operated at a scan rate of 240 nm/min at 25 °C. The solution of EL and the EL–3-NPBA complex were excited at 388 nm for fluorescence measurements. The fluorescence spectra of EL or the EL–3-NPBA complex by adding metal ions were recorded within the wavelength range from 410 to 700 nm. The slits of both excitation and emission were set to 10 nm. The excitation wavelength was determined by the isosbestic point in the UV-vis titration of EL for 3-NPBA. A Hamamatsu Photonics Quantaaurus-QY C11347-01 and the Hamamatsu Photonics Quantaaurus-Tau C11367-01 with a quartz cuvette (Hamamatsu Photonics A10095-02, 10 × 10 mm) were applied to measure the absolute fluorescence quantum yields (φ) and the lifetimes (τ), respectively. All array experiments in the solution states were carried out using a Biotek SYNERGY H1M microplate reader. Each experiment was replicated 24 times. A mixture solution (100 μL) containing EL (4 μM), 3-NPBA (240 μM), and a target metal ion was added to each well of 384-well microtiter plastic plates (Thermo Scientific™, Black 384-Well Immuno Plates, No. 460518). The mixture solutions in the 384-well microtiter plastic plate were excited at 388 nm, and the gain was set to 100. The fluorescence spectra of the mixtures were recorded from 410 to 700 nm.

ESI-MS Analysis: Electrospray ionization-mass spectrometry (ESI-MS) was carried out using a Shimadzu LC-2010CHT and a Shimadzu LCMS-2020 controlled by Shimadzu LabSolutions. The ESI-MS was operated by scan mode with interface potential at +4.5 kV, the flow rate of nebulizer N_2 gas at 1.5 L/min, the capillary temperature of 500 °C, and Qarray RF voltage at 60 V.

NMR Analysis: NMR measurement was conducted using a JEOL ECZ-600 spectrometer with solvent peaks as internal standards. The pD of the solutions was adjusted using NaOD and DCl, which was determined using a HORIBA LAQUAtwin pH-22B pH meter.

Methods

Data processing: Linear discriminant analysis (LDA) for the semi-quantitative assay was carried out using SYSTAT 13 without any further data treatment. Support vector machine (SVM) with Solo 9.0. was performed for the quantitative analysis of river water.

2. UV-vis and fluorescence titrations of 3-NPBA

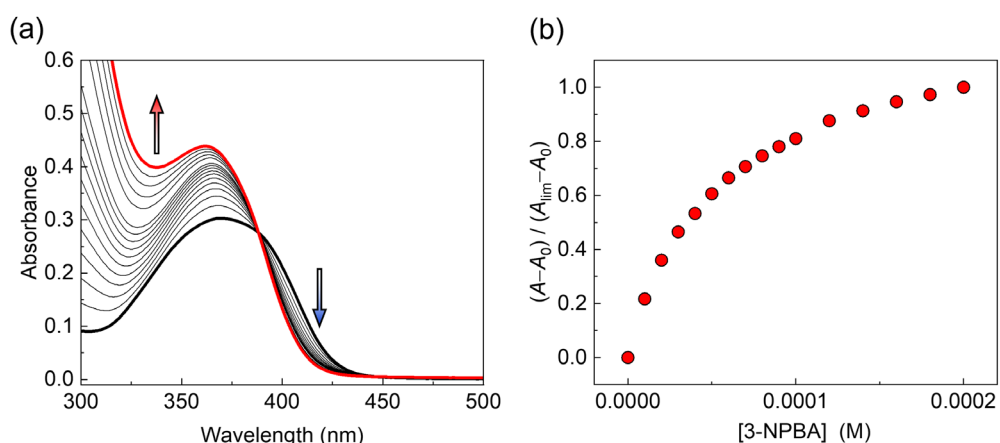


Fig. S1 (a) Changes in UV-vis absorption spectra of EL (40 μM) upon adding 3-NPBA in a HEPES buffer (50 mM) at pH 7.4 at 25 $^\circ\text{C}$. (b) Titration isotherm for 3-NPBA. The titration isotherm was obtained by plotting the maximum absorbance at 370 nm. $[3\text{-NPBA}] = 0 - 200 \mu\text{M}$.

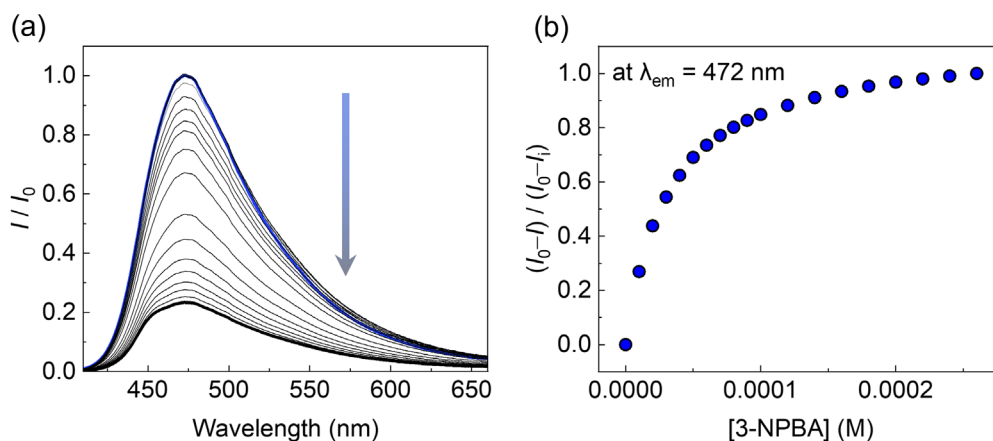


Fig. S2 (a) Changes in fluorescence spectra of EL (4 μM) upon adding 3-NPBA in a HEPES buffer (50 mM) at pH 7.4 at 25 $^\circ\text{C}$. (b) The titration isotherm for 3-NPBA were obtained by plotting the emission at 472 nm. $[3\text{-NPBA}] = 0 - 260 \mu\text{M}$. $\lambda_{ex} = 388 \text{ nm}$.

3. Selected UV-vis titrations

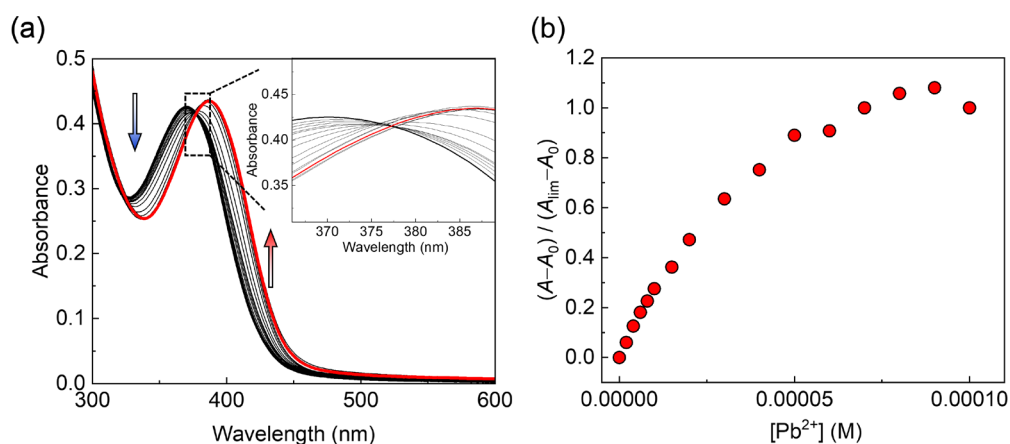


Fig. S3 (a) Changes in UV-vis absorption spectra of EL (40 μM) with 3-NPBA (80 μM) upon adding Pb^{2+} in a HEPES buffer (50 mM) at pH 7.4 at 25 $^{\circ}\text{C}$. (b) Titration isotherm for Pb^{2+} . The titration isotherm was obtained by plotting the maximum absorbance at 369 nm. $[\text{Pb}^{2+}] = 0 - 100 \mu\text{M}$.

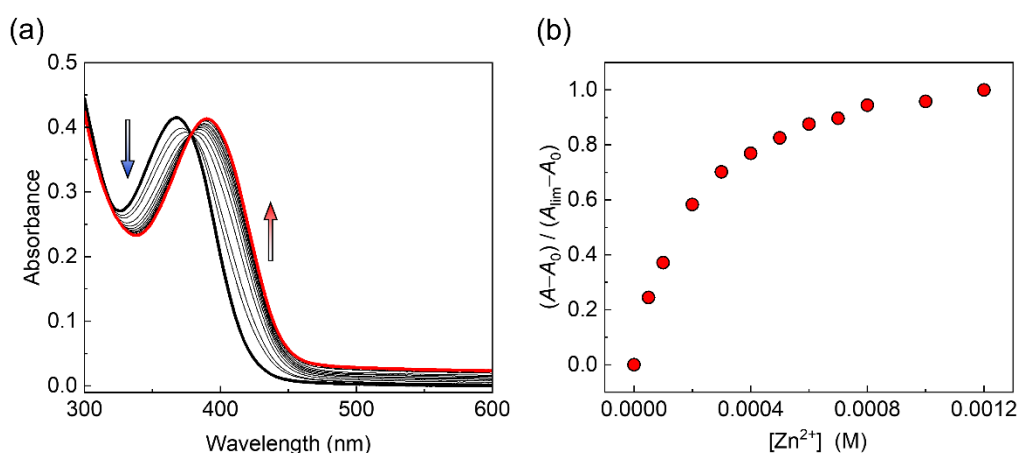


Fig. S4 (a) Changes in UV-vis absorption spectra of EL (40 μM) with 3-NPBA (80 μM) upon adding Zn^{2+} in a HEPES buffer (50 mM) at pH 7.4 at 25 $^{\circ}\text{C}$. (b) Titration isotherm for Zn^{2+} . The titration isotherm was obtained by plotting the maximum absorbance at 369 nm. $[\text{Zn}^{2+}] = 0 - 1200 \mu\text{M}$.

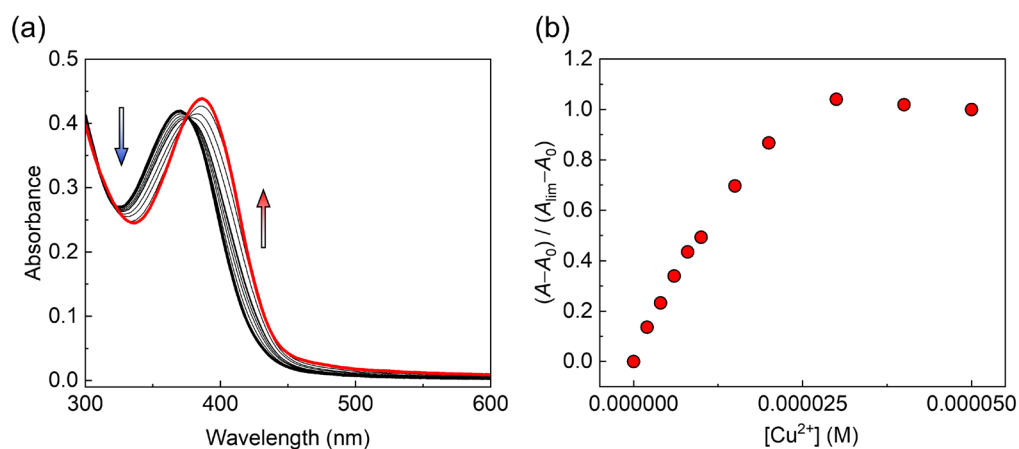


Fig. S5 (a) Changes in UV-vis absorption spectra of EL (40 μM) with 3-NPBA (80 μM) upon adding Cu^{2+} in a HEPES buffer (50 mM) at pH 7.4 at 25 $^{\circ}\text{C}$. (b) Titration isotherm for Cu^{2+} . The titration isotherm was obtained by plotting the maximum absorbance at 369 nm. $[\text{Cu}^{2+}] = 0 - 50 \mu\text{M}$.

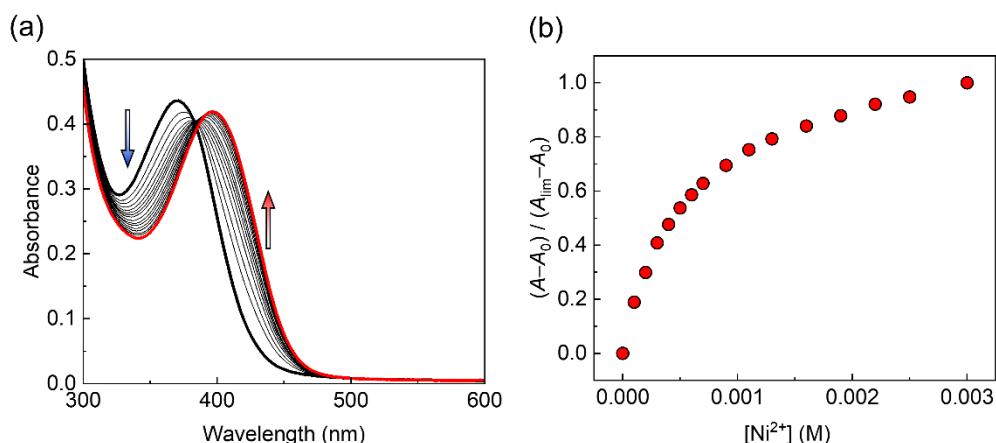


Fig. S6 (a) Changes in UV-vis absorption spectra of EL (40 μM) with 3-NPBA (80 μM) upon adding Ni^{2+} in a HEPES buffer (50 mM) at pH 7.4 at 25 $^{\circ}\text{C}$. (b) Titration isotherm for Ni^{2+} . The titration isotherm was obtained by plotting the maximum absorbance at 369 nm. $[\text{Ni}^{2+}] = 0 - 3000 \mu\text{M}$.

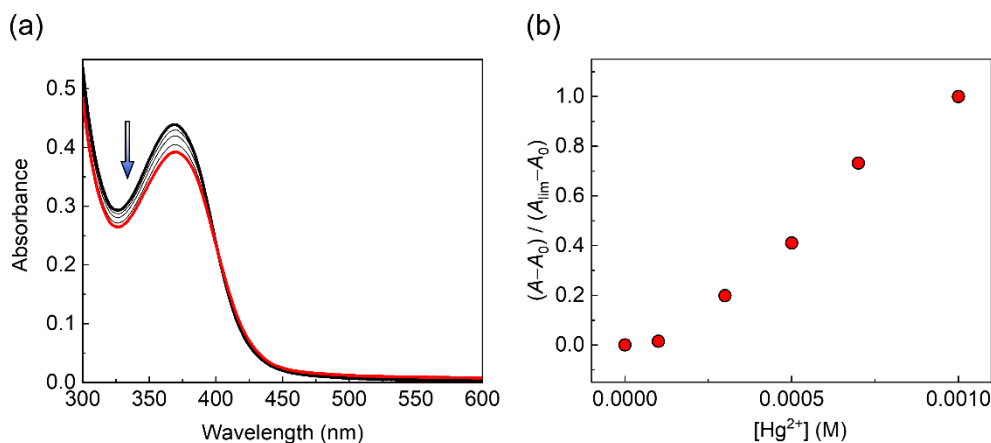


Fig. S7 (a) Changes in UV-vis absorption spectra of EL (40 μM) with 3-NPBA (80 μM) upon adding Hg^{2+} in a HEPES buffer (50 mM) at pH 7.4 at 25 $^{\circ}\text{C}$. (b) Titration isotherm for Hg^{2+} . The titration isotherm was obtained by plotting the maximum absorbance at 369 nm. $[\text{Hg}^{2+}] = 0 - 1000 \mu\text{M}$. The titration was conducted up to 1000 μM because of a precipitation at high concentrations.

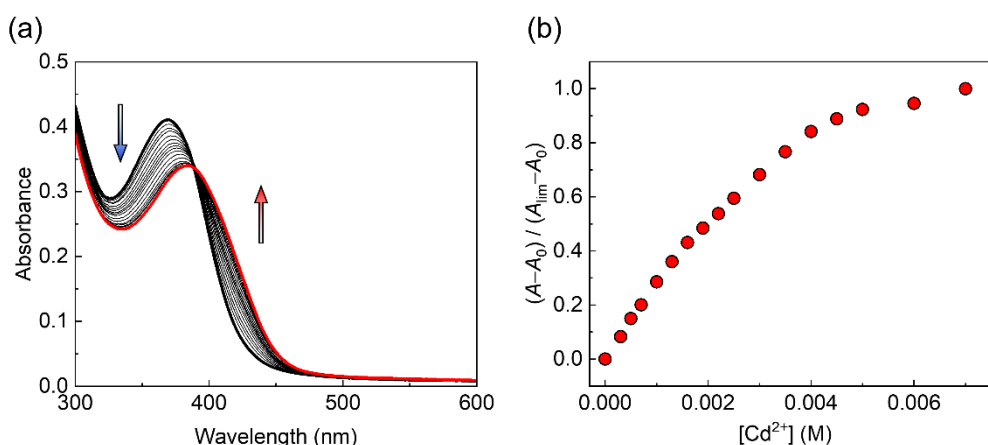


Fig. S8 (a) Changes in UV-vis absorption spectra of EL (40 μM) with 3-NPBA (80 μM) upon adding Cd^{2+} in a HEPES buffer (50 mM) at pH 7.4 at 25 $^{\circ}\text{C}$. (b) Titration isotherm for Cd^{2+} . The titration isotherm was obtained by plotting the maximum absorbance at 369 nm. $[\text{Cd}^{2+}] = 0 - 7000 \mu\text{M}$.

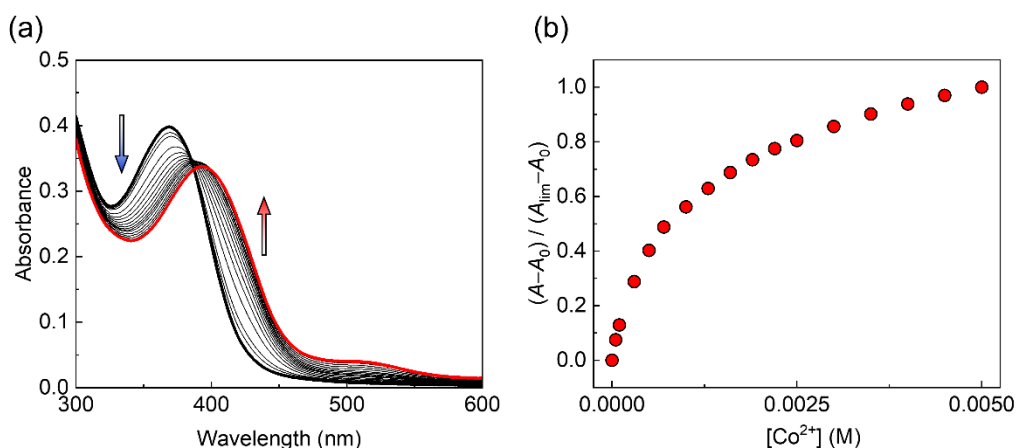


Fig. S9 (a) Changes in UV-vis absorption spectra of EL (40 μM) with 3-NPBA (80 μM) by adding Co^{2+} in a HEPES buffer (50 mM) at pH 7.4 at 25 $^{\circ}\text{C}$. (b) Titration isotherm for Co^{2+} . The titration isotherm was obtained by plotting the maximum absorbance at 369 nm. $[\text{Co}^{2+}] = 0 - 5000 \mu\text{M}$.

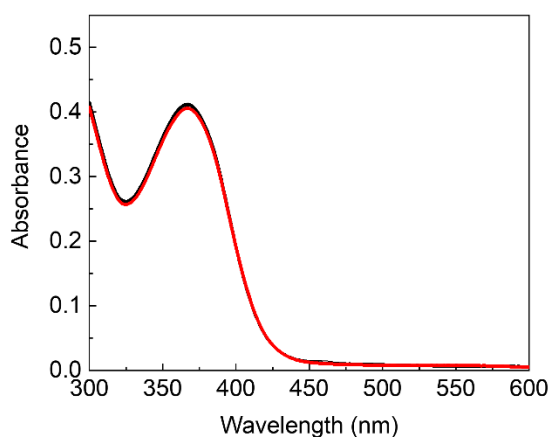


Fig. S10 UV-vis absorption spectra of EL (40 μM) with 3-NPBA (80 μM) upon adding Ca^{2+} in a HEPES buffer (50 mM) at pH 7.4 at 25 $^{\circ}\text{C}$. $[\text{Ca}^{2+}] = 0 - 1000 \mu\text{M}$.

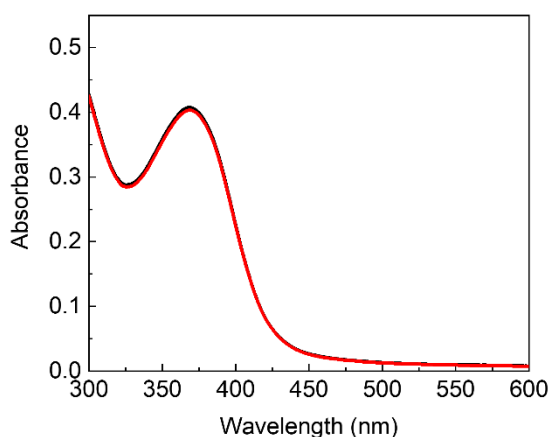


Fig. S11 UV-vis absorption spectra of EL (40 μM) with 3-NPBA (80 μM) upon adding K^{+} in a HEPES buffer (50 mM) at pH 7.4 at 25 $^{\circ}\text{C}$. $[\text{K}^{+}] = 0 - 1000 \mu\text{M}$.

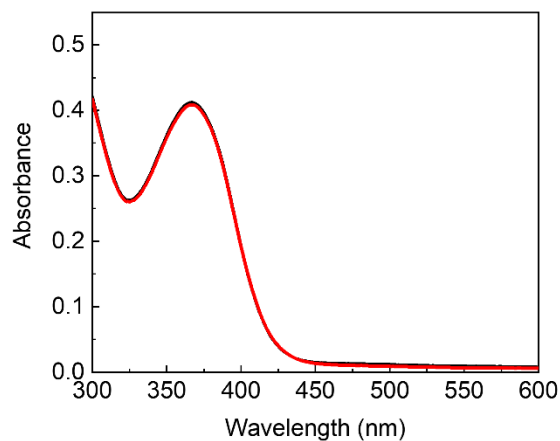


Fig. S12 UV-vis absorption spectra of EL (40 μM) with 3-NPBA (80 μM) upon adding Na^+ in a HEPES buffer (50 mM) at pH 7.4 at 25 $^{\circ}\text{C}$. [Na^+] = 0 – 1000 μM .

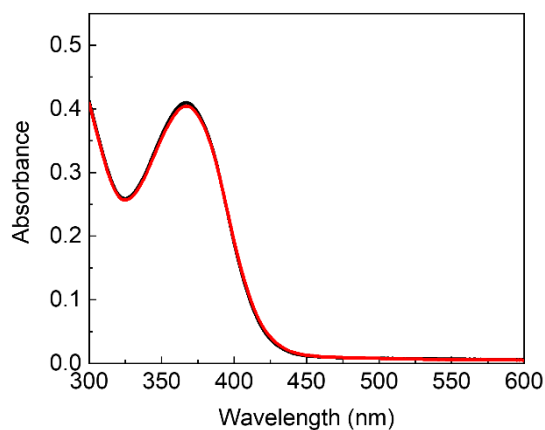


Fig. S13 UV-vis absorption spectra of EL (40 μM) with 3-NPBA (80 μM) upon adding Mg^{2+} in a HEPES buffer (50 mM) at pH 7.4 at 25 $^{\circ}\text{C}$. [Mg^{2+}] = 0 – 1000 μM .

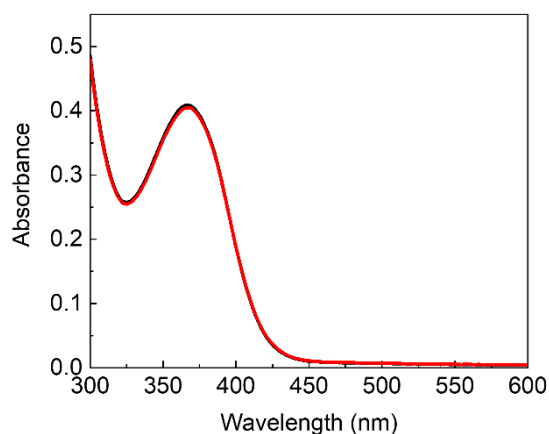


Fig. S14 UV-vis absorption spectra of EL (40 μM) with 3-NPBA (80 μM) upon adding Ba^{2+} in a HEPES buffer (50 mM) at pH 7.4 at 25 $^{\circ}\text{C}$. [Ba^{2+}] = 0 – 1000 μM .

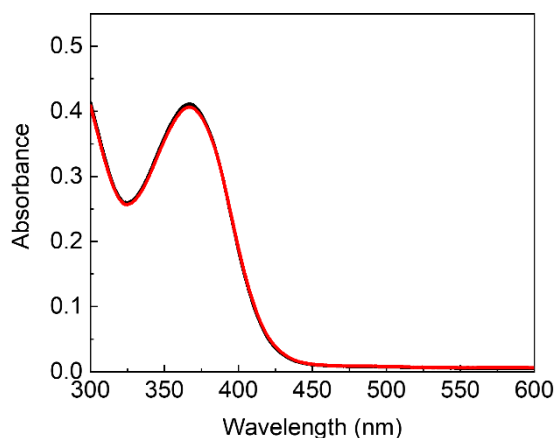


Fig. S15 UV-vis absorption spectra of EL (40 μM) with 3-NPBA (80 μM) upon adding Cs^+ in a HEPES buffer (50 mM) at pH 7.4 at 25 $^{\circ}\text{C}$. $[\text{Cs}^+] = 0 - 1000 \mu\text{M}$.

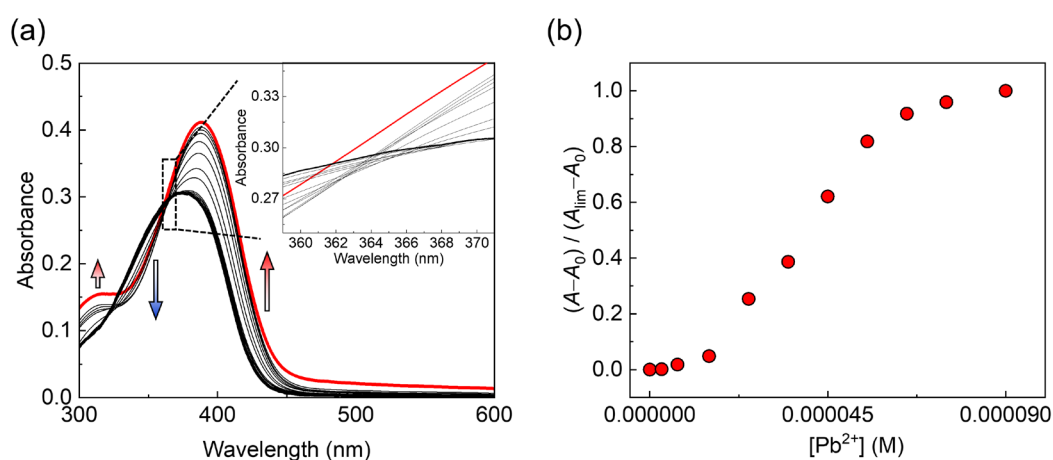


Fig. S16 (a) Changes in UV-vis absorption spectra of EL (40 μM) upon adding Pb^{2+} in a HEPES buffer (50 mM) at pH 7.4 at 25 $^{\circ}\text{C}$. (b) Titration isotherm for Pb^{2+} . The titration isotherm was obtained by plotting the maximum absorbance at 376 nm. $[\text{Pb}^{2+}] = 0 - 90 \mu\text{M}$.

4. Selected fluorescence titrations

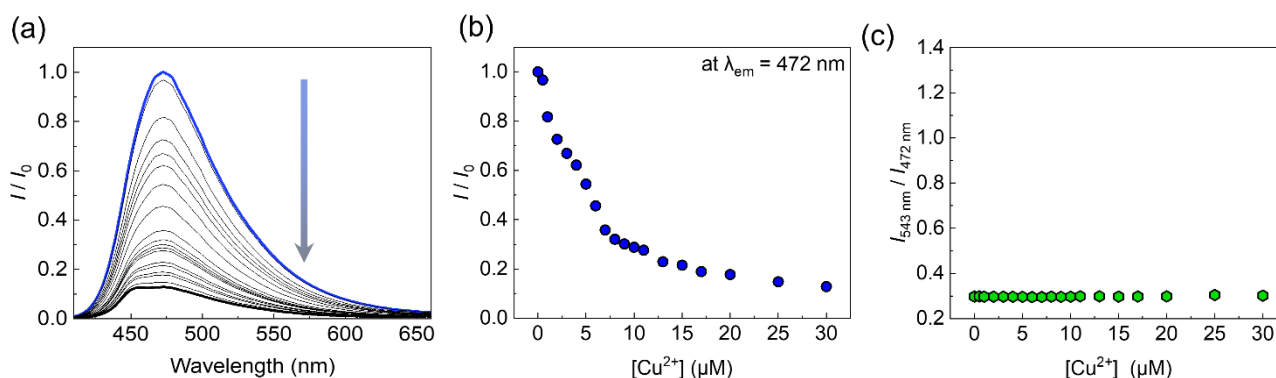


Fig. S17 (a) Changes in fluorescence spectra of EL (4 μM) with 3-NPBA (240 μM) upon adding Cu^{2+} in a HEPES buffer (50 mM) at pH 7.4 at 25 $^{\circ}\text{C}$. $\lambda_{\text{ex}} = 388 \text{ nm}$. (b) The titration isotherm for Cu^{2+} obtained by plotting the emission at 472 nm. (c) Emission ratio ($I_{543 \text{ nm}} / I_{472 \text{ nm}}$) of EL-3-NPBA upon adding Cu^{2+} . $[\text{Cu}^{2+}] = 0 - 30 \mu\text{M}$.

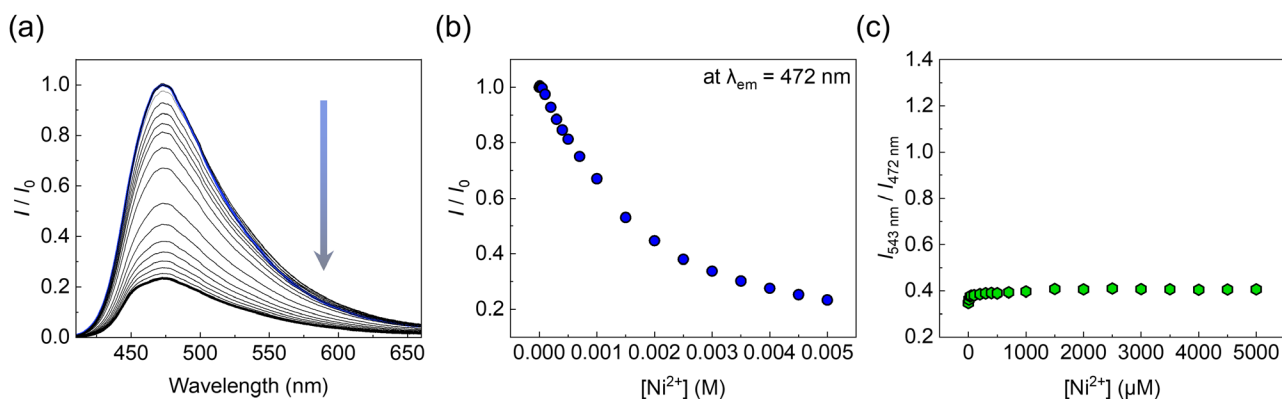


Fig. S18 (a) Changes in fluorescence spectra of EL (4 μM) with 3-NPBA (240 μM) upon adding Ni^{2+} in a HEPES buffer (50 mM) at pH 7.4 at 25 $^{\circ}\text{C}$. $\lambda_{\text{ex}} = 388$ nm. (b) The titration isotherms for Ni^{2+} obtained by plotting the emission at 472 nm. (c) Emission ratio ($I_{543 \text{ nm}} / I_{472 \text{ nm}}$) of EL-3-NPBA upon adding Ni^{2+} . [Ni^{2+}] = 0 – 5000 μM .

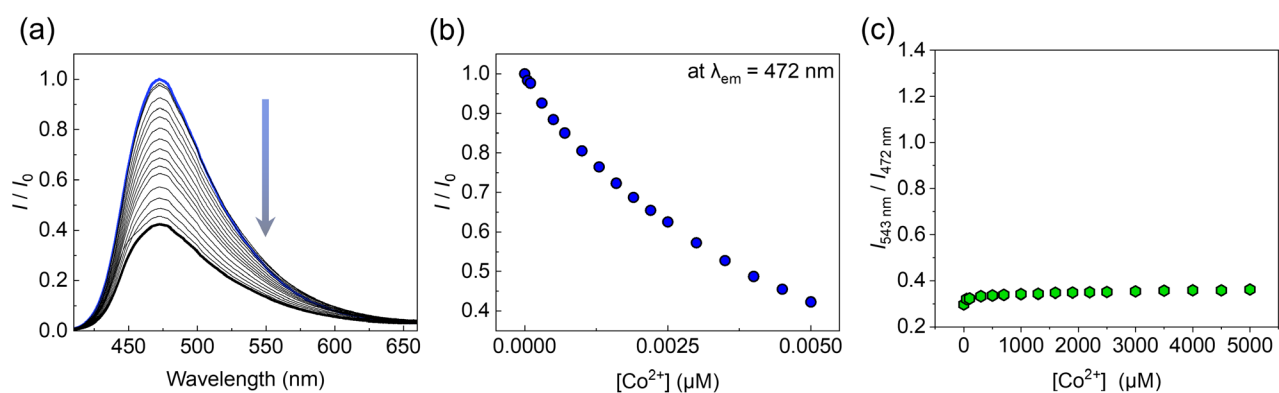


Fig. S19 (a) Changes in fluorescence spectra of EL (4 μM) with 3-NPBA (240 μM) upon adding Co^{2+} in a HEPES buffer (50 mM) at pH 7.4 at 25 $^{\circ}\text{C}$. $\lambda_{\text{ex}} = 388$ nm. (b) The titration isotherms for Co^{2+} obtained by plotting the emission at 472 nm. (c) Emission ratio ($I_{543 \text{ nm}} / I_{472 \text{ nm}}$) of EL-3-NPBA upon adding Co^{2+} . [Co^{2+}] = 0 – 5000 μM .

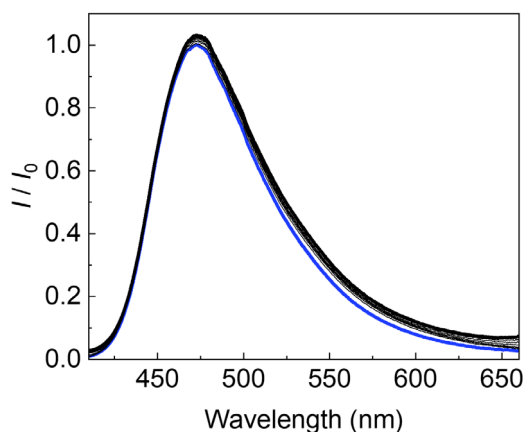


Fig. S20 Fluorescence spectra of EL (4 μM) with 3-NPBA (240 μM) upon adding Hg^{2+} in a HEPES buffer (50 mM) at pH 7.4 at 25 $^{\circ}\text{C}$. [Hg^{2+}] = 0 – 1000 μM . $\lambda_{\text{ex}} = 388$ nm.

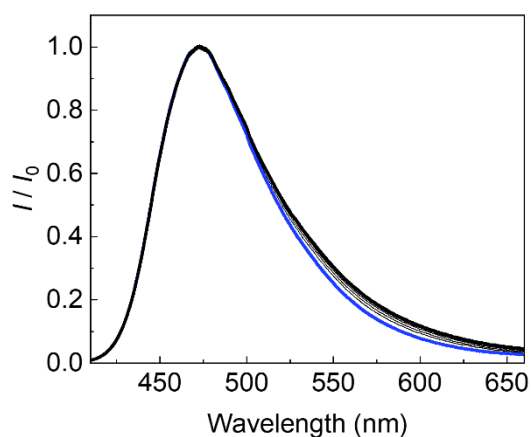


Fig. S21 Fluorescence spectra of EL (4 μM) with 3-NPBA (240 μM) upon adding Cd^{2+} in a HEPES buffer (50 mM) at pH 7.4 at 25 $^{\circ}\text{C}$. $[\text{Cd}^{2+}] = 0 - 1000 \mu\text{M}$. $\lambda_{\text{ex}} = 388 \text{ nm}$.

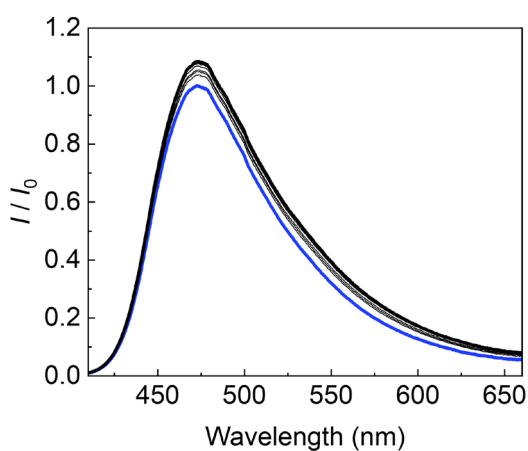


Fig. S22 (a) Fluorescence spectra of EL (4 μM) with 3-NPBA (240 μM) upon adding Ca^{2+} in a HEPES buffer (50 mM) at pH 7.4 at 25 $^{\circ}\text{C}$. $[\text{Ca}^{2+}] = 0 - 1000 \mu\text{M}$. $\lambda_{\text{ex}} = 388 \text{ nm}$.

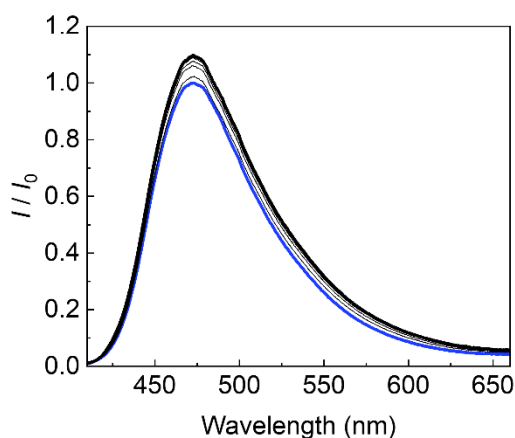


Fig. S23 (a) Fluorescence spectra of EL (4 μM) with 3-NPBA (240 μM) upon adding K^{+} in a HEPES buffer (50 mM) at pH 7.4 at 25 $^{\circ}\text{C}$. $[\text{K}^{+}] = 0 - 1000 \mu\text{M}$. $\lambda_{\text{ex}} = 388 \text{ nm}$.

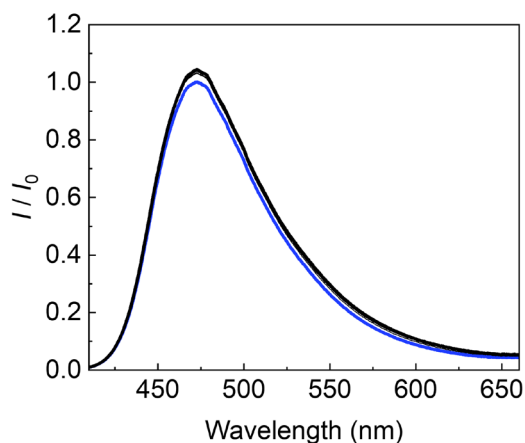


Fig. S24 (a) Fluorescence spectra of EL (4 μM) with 3-NPBA (240 μM) upon adding Na^+ in a HEPES buffer (50 mM) at pH 7.4 at 25 $^\circ\text{C}$. [Na^+] = 0 – 1000 μM . λ_{ex} = 388 nm.

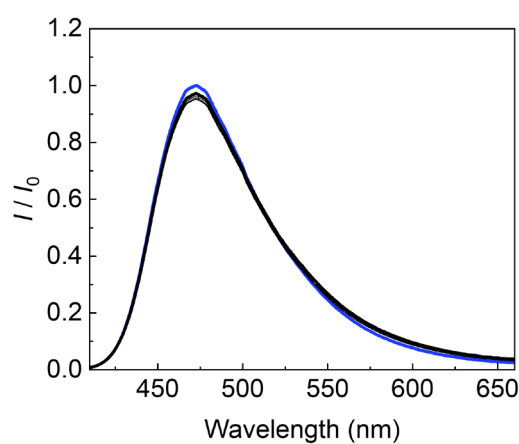


Fig. S25 (a) Fluorescence spectra of EL (4 μM) with 3-NPBA (240 μM) upon adding Mg^{2+} in a HEPES buffer (50 mM) at pH 7.4 at 25 $^\circ\text{C}$. [Mg^{2+}] = 0 – 1000 μM . λ_{ex} = 388 nm.

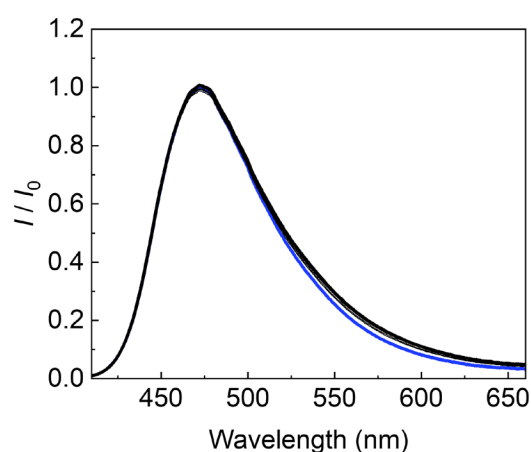


Fig. S26 (a) Fluorescence spectra of EL (4 μM) with 3-NPBA (240 μM) upon adding Ba^{2+} in a HEPES buffer (50 mM) at pH 7.4 at 25 $^\circ\text{C}$. [Ba^{2+}] = 0 – 1000 μM . λ_{ex} = 388 nm.

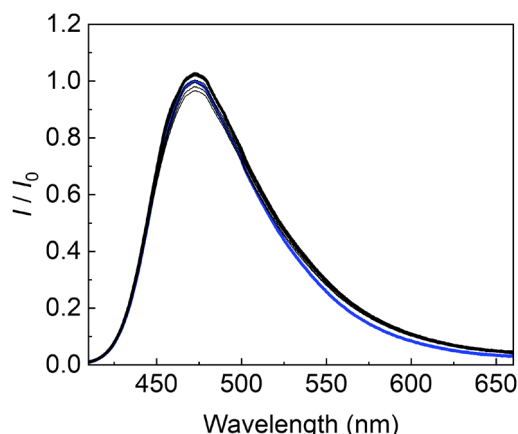


Fig. S27 (a) Fluorescence spectra of EL (4 μM) with 3-NPBA (240 μM) upon adding Cs^+ in a HEPES buffer (50 mM) at pH 7.4 at 25 $^\circ\text{C}$. $[\text{Cs}^+] = 0 - 1000 \mu\text{M}$. $\lambda_{\text{ex}} = 388 \text{ nm}$.

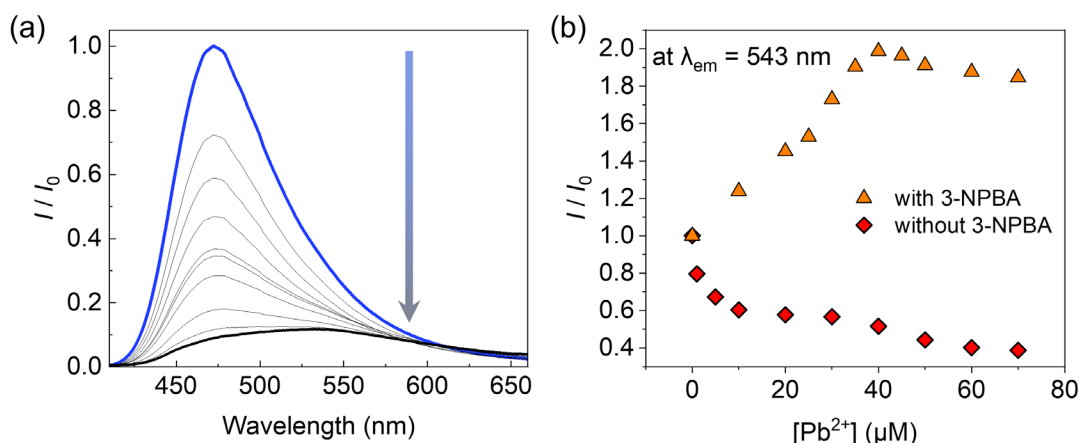


Fig. S28 (a) Changes in fluorescence spectra of EL (4 μM) upon adding Pb^{2+} in a HEPES buffer (50 mM) at pH 7.4 at 25 $^\circ\text{C}$. $[\text{Pb}^{2+}] = 0 - 80 \mu\text{M}$. $\lambda_{\text{ex}} = 473 \text{ nm}$. (b) The titration isotherms for Pb^{2+} with and without 3-NPBA obtained by plotting the maximum emission at 543 nm.

5. Emission quantum yield and emission lifetime

Table S1. The emission quantum yield (Φ) and emission lifetime (τ) of EL and its complexes

	EL	EL- Pb^{2+}	EL-3NPBA	EL-3NPBA with Pb^{2+}
Φ (%)	21	< 1.0	3.0	1.9
τ_1 (ns)	2.17	0.27 (76%)	< 0.1 (68%)	0.25 (78%)
τ_2 (ns)	-	2.28 (24%)	2.12 (32%)	2.14 (22%)

$[\text{EL}] = 4 \mu\text{M}$, $[\text{3-NPBA}] = 240 \mu\text{M}$, $[\text{Pb}^{2+}] = 40 \mu\text{M}$ in a 50 mM HEPES buffer solution at pH 7.4. λ_{ex} for $\Phi = 388 \text{ nm}$. λ_{ex} for $\tau = 365 \text{ nm}$.

6. Discuss on a binding stoichiometry between EL and Pb^{2+}

As shown in Fig. S3, the UV-vis absorption spectra of EL in the presence of 3-NPBA showed redshifts upon the addition of Pb^{2+} . In addition, the isosbestic point was slightly shifted with an increase in Pb^{2+} concentration (Fig. S3, inset). In the absence of 3-NPBA, the UV-vis absorption spectra of EL showed biphasic behavior with an increase in Pb^{2+} concentration (Fig. S16, inset). Thus, the abovementioned results in Figs. S3 and S16 implied the multi-equilibria in the coordination of EL and Pb^{2+} .^{2,3}

7. Semi-quantitative assay

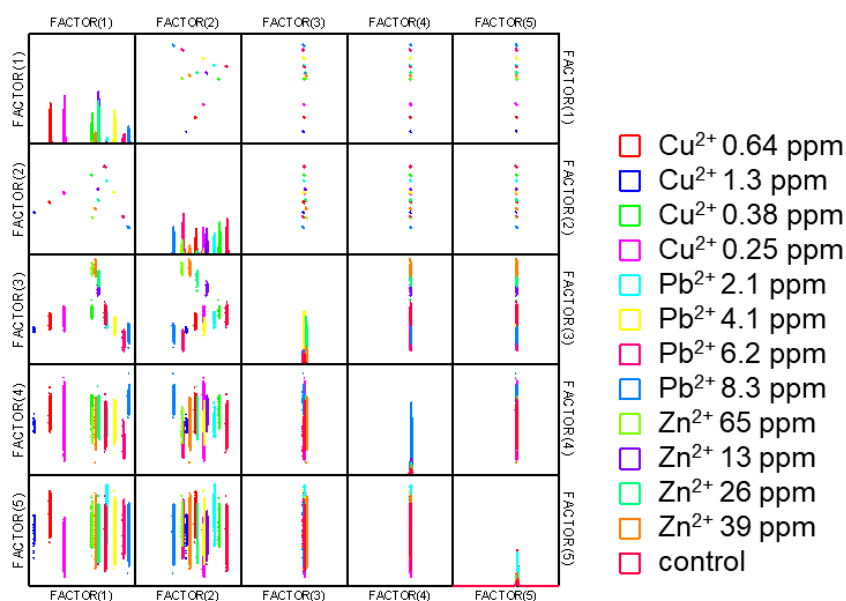


Fig. S29 The canonical score plot of the semi-quantitative assay for Cu^{2+} , Zn^{2+} , and Pb^{2+} .

Table S2. The jackknifed classification matrix of the semi-quantitative assay for Cu^{2+} , Zn^{2+} , and Pb^{2+}

	Cu^{2+} _0.64 ppm	Cu^{2+} _1.3 ppm	Cu^{2+} _0.25 ppm	Cu^{2+} _0.38 ppm	Pb^{2+} _2.1 ppm	Pb^{2+} _4.1 ppm	Pb^{2+} _6.2 ppm	Pb^{2+} _8.3 ppm	Zn^{2+} _65 ppm	Zn^{2+} _13 ppm	Zn^{2+} _26 ppm	Zn^{2+} _39 ppm	control	%correct
Cu^{2+} _0.64 ppm	20	0	0	0	0	0	0	0	0	0	0	0	0	100
Cu^{2+} _1.3 ppm	0	20	0	0	0	0	0	0	0	0	0	0	0	100
Cu^{2+} _0.25 ppm	0	0	20	0	0	0	0	0	0	0	0	0	0	100
Cu^{2+} _0.38 ppm	0	0	0	20	0	0	0	0	0	0	0	0	0	100
Pb^{2+} _2.1 ppm	0	0	0	0	20	0	0	0	0	0	0	0	0	100
Pb^{2+} _4.1 ppm	0	0	0	0	0	20	0	0	0	0	0	0	0	100
Pb^{2+} _6.2 ppm	0	0	0	0	0	0	20	0	0	0	0	0	0	100
Pb^{2+} _8.3 ppm	0	0	0	0	0	0	0	20	0	0	0	0	0	100
Zn^{2+} _65 ppm	0	0	0	0	0	0	0	0	20	0	0	0	0	100
Zn^{2+} _13 ppm	0	0	0	0	0	0	0	0	0	20	0	0	0	100
Zn^{2+} _26 ppm	0	0	0	0	0	0	0	0	0	0	20	0	0	100
Zn^{2+} _39 ppm	0	0	0	0	0	0	0	0	0	0	0	20	0	100
control	0	0	0	0	0	0	0	0	0	0	0	0	20	100
Total	20	20	20	20	20	20	20	20	20	20	20	20	20	100

8. Real-sample analysis

Table S3. The elements of the original river water sample

Element	Concentration
B	44.0 $\mu\text{g}/\text{kg}$
Al	21.8 $\mu\text{g}/\text{kg}$
Cr	5.16 $\mu\text{g}/\text{kg}$
Mn	5.04 $\mu\text{g}/\text{kg}$
Fe	27.1 $\mu\text{g}/\text{kg}$
Ni	1.06 $\mu\text{g}/\text{kg}$

Cu	10.1 µg/kg
Zn	10.6 µg/kg
As	1.17 µg/kg
Se	1.03 µg/kg
Rb	0.653 µg/kg
Sr	33.5 µg/kg
Mo	0.183 µg/kg
Cd	1.01 µg/kg
Sb	0.0095 µg/kg
Ba	5.74 µg/kg
Pb	1.018 µg/kg
Na	3.68 mg/kg
Mg	1.26 mg/kg
K	0.836 mg/kg
Ca	4.59 mg/kg

References

1. J. R. Lakowicz, Principles of Fluorescence Spectroscopy 3rd Ed., Springer, New York, USA, 2006.
2. S. C. McCleskey, A. Metzger, C. S. Simmons and E. V. Anslyn, *Tetrahedron*, 2002, **58**, 621-628.
3. A. Le Person, A. Moncombe and J.-P. Cornard, *J. Phys. Chem. A*, 2014, **118**, 2646-2655.